

Combined synchrotron and nonlinear SSC cooling of relativistic electrons

Reinhard Schlickeiser

Institut für Theoretische Physik

Lehrstuhl IV: Weltraum- und Astrophysik

Ruhr-Universität Bochum, Germany

June 21, 2010



Introduction

Linear synchrotron . . .

Intrinsic optically . . .

Synchrotron and . . .

Comparison with . . .

Summary and . . .

Topics:

1. Introduction
2. Linear synchrotron and nonlinear SST electron cooling
3. Intrinsic optically thin synchrotron radiation intensities and fluences
4. SEDs from numerical radiation code
5. Comparison with observations and future work
6. Summary and conclusions

Collaborators: M. Böttcher, U. Menzler, M. Zacharias

References:

Combined synchrotron and nonlinear synchrotron-self-Compton cooling of relativistic electrons, R. Schlickeiser, M. Böttcher and U. Menzler, 2010, *Astron. Astrophys.*, in press

Nonlinear synchrotron self-Compton cooling of relativistic electrons; R. Schlickeiser, 2009, *MNRAS* 398, 1483.



Introduction

Linear synchrotron . . .

Intrinsic optically . . .

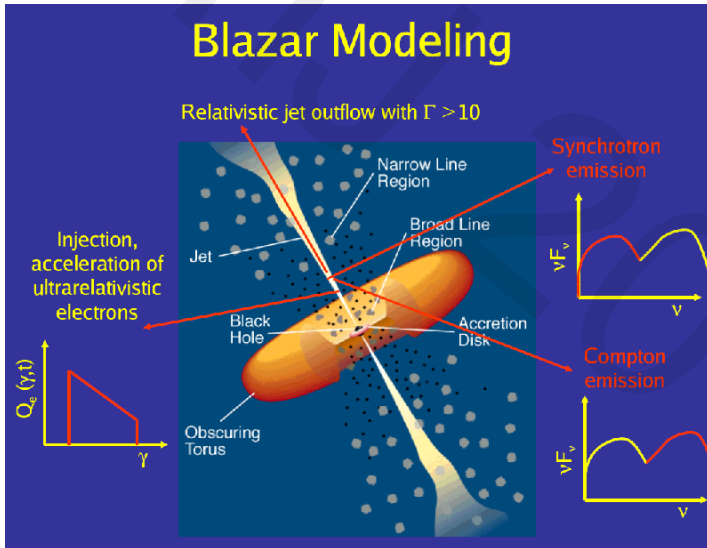
Synchrotron and . . .

Comparison with . . .

Summary and . . .

1. Introduction

The broadband SEDs of blazars exhibit two broad spectral components. In leptonic models the low-energy component is attributed to synchrotron radiation of relativistic electrons whereas the high-energy component results from synchrotron-self Compton (SSC) interactions of the relativistic electrons, inverse Compton upscattering the synchrotron photons.



Introduction

Linear synchrotron ...

Intrinsic optically ...

Synchrotron and ...

Comparison with ...

Summary and ...

The Fermi survey of blazars (Abdo et al. 2010) and multiwavelength monitoring of the individual blazars PKS 0528+134 (Aharonian et al. 2005), 1ES 1121-232 (Aharonian et al. 2007b), PKS 0528+134 (Sambruna et al. 1997) and Mrk 421 (Fossati et al. 2008) have shown that basically two types of blazars exist:

(a) Synchrotron-dominated blazars where $L_S \gg L_{SSC}$, corresponding to $|\dot{\gamma}_S| \gg |\dot{\gamma}_{SSC}|$,

(b) Compton-dominated blazars where $L_{SSC} \gg L_S$, corresponding to $|\dot{\gamma}_{SSC}| \gg |\dot{\gamma}_S|$,

because of the identical Doppler boosting factors of synchrotron and SSC emission:

$$L_S = mc^2 \int dV \int_1^\infty d\gamma n(\gamma) |\dot{\gamma}_S|,$$

$$L_{SSC} = mc^2 \int dV \int_1^\infty d\gamma n(\gamma) |\dot{\gamma}_{SSC}| \quad (1)$$

All physical quantities are calculated in a coordinate system comoving with the radiation source.



Introduction

Linear synchrotron ...

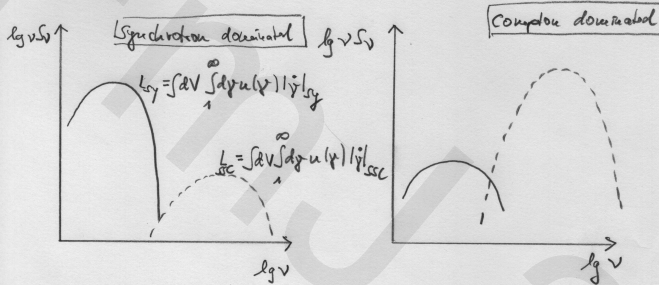
Intrinsic optically ...

Synchrotron and ...

Comparison with ...

Summary and ...

2 types of blazars



In synchrotron-dominated sources:

$$|j|_{SSC} \ll |j|_{SY} = \frac{4}{3} \frac{c\sigma_T}{mc^2} U_B \gamma^2$$

In Compton-dominated sources:

$$|j|_{SY} \ll |j|_{SSC} = \frac{3\sigma_T c_1 P_0 R_0^2}{4\pi mc^2} \underbrace{\int_1^\infty d\gamma \gamma^2 u(\gamma)}_{\text{nonlinear behavior!}}$$



Introduction

Linear synchrotron ...

Intrinsic optically ...

Synchrotron and ...

Comparison with ...

Summary and ...

2. Linear synchrotron and nonlinear SST electron cooling

The competition between the instantaneous injection of ultrarelativistic electrons ($\gamma_0 \gg 1$) at the rate $Q(\gamma, t) = q_0 \delta(\gamma - \gamma_0) \delta(t)$ at time $t = 0$ and the electron synchrotron energy losses is described by the time-dependent kinetic equation for the volume-averaged relativistic electron population inside the radiating source (Kardashev 1962):

$$\frac{\partial n(\gamma, t)}{\partial t} - \frac{\partial}{\partial \gamma} [|\dot{\gamma}| n(\gamma, t)] = q_0 \delta(\gamma - \gamma_0) \delta(t) \quad (2)$$

2.1. Linear synchrotron cooling only

With

$$|\dot{\gamma}|_S = D_0 \gamma^2, \quad D_0 = \frac{4}{3} \frac{c \sigma_T}{m c^2} U_B = 1.29 \cdot 10^{-9} b^2 \text{ s}^{-1} \quad (3)$$

the solution of this kinetic equation is (H denotes Heaviside step function)

$$n_S(\gamma, \gamma_0, t) = q_0 H[\gamma_0 - \gamma] \delta(\gamma - \gamma_S(t)), \quad \gamma_S(t) = \frac{\gamma_0}{1 + D_0 \gamma_0 t} \quad (4)$$

The half-life time, t_s is

$$t_s = \frac{1}{D_0 \gamma_0} = \frac{7.75 \cdot 10^4}{\gamma_4 b^2} \text{ s} \quad (5)$$



Introduction

Linear synchrotron ...

Intrinsic optically ...

Synchrotron and ...

Comparison with ...

Summary and ...

2.2. Combined linear synchrotron and nonlinear SST cooling

For combined synchrotron and SST cooling the kinetic equation (6) reads with the substitution $y = A_0 t$

$$\frac{\partial n(\gamma, t)}{\partial y} - \frac{\partial}{\partial \gamma} \left[\gamma^2 n(\gamma, t) \left(K_0 + \int_0^\infty d\tilde{\gamma} \tilde{\gamma}^2 n(\tilde{\gamma}, t) \right) \right] = q_0 \delta(\gamma - \gamma_0) \delta(y) \quad (6)$$

where $K_0 = D_0/A_0$. We set $S = \gamma^2 n$ and use $x = 1/\gamma$ as independent variable to obtain

$$\frac{\partial S}{\partial y} + \frac{\partial S}{\partial x} \left[K_0 + \int_0^\infty d\tilde{x} \tilde{x}^{-2} S(\tilde{x}, y) \right] = q_0 \delta(x - x_0) \delta(y) \quad (7)$$

Now we define the implicit time variable T through

$$\frac{dT}{dy} = U(y) = K_0 + \int_0^\infty dx x^{-2} S(x, y) \quad (8)$$

Then Eq. (7) becomes

$$\frac{\partial S}{\partial T} + \frac{\partial S}{\partial x} = q_0 \delta(x - x_0) \delta(T) \quad (9)$$

which is solved by the method of characteristics (or double Laplace transform) as



Introduction

Linear synchrotron ...

Intrinsic optically ...

Synchrotron and ...

Comparison with ...

Summary and ...

$$S(x, T) = q_0 \delta(x - T - x_0) (H[T] - H[T - x]) \quad (10)$$

The final step is then to calculate explicitly the time variable T as a function of y . Use Eq. (10) in Eq. (8) to write

$$\frac{dT}{dy} = K_0 + \int_0^\infty dx x^{-2} S(x, y) = K_0 + \frac{q_0}{(x_0 + T)^2} \quad (11)$$

for $x_0 > 0$ and $T \geq 0$. The solution of Eq. (11) with the condition that $T = 0$ for $y = 0$ is

$$K_0 y = T - \sqrt{\frac{q_0}{K_0}} \left[\arctan \left(\sqrt{\frac{K_0}{q_0}} [x_0 + T(y)] \right) - \arctan \left(\sqrt{\frac{K_0}{q_0}} x_0 \right) \right] \quad (12)$$

Unfortunately, for $K_0 \neq 0$ this dependence $y(T)$ cannot be inverted to infer the general dependence $T(y)$. However, an approximate inversion is possible.

2.2.1. Injection parameter

The arguments of the arctan-function are always larger than $\alpha^{-1} = x_0(K_0/q_0)^{1/2}$. Therefore, we have to consider the two cases $\alpha \geq 1$ and $\alpha < 1$, respectively, where $\alpha = 46\gamma_4 N_{50}^{1/2} / R_{15} = \gamma_0 / \gamma_B$, $\gamma_B = 217 R_{15} / N_{50}^{1/2}$. Obviously, the more compact the source is, and the more electrons are injected, the smaller the characteristic Lorentz factor γ_B is. If the injection Lorentz factor γ_0 is higher



Introduction

Linear synchrotron ...

Intrinsic optically ...

Synchrotron and ...

Comparison with ...

Summary and ...

(smaller) than γ_B , the injection parameter α will be larger (smaller) than unity. For a compact sources with a large number of injected relativistic electrons the injection parameter α is much larger than unity. For small values of the injection parameter $\alpha < 1$, corresponding to $\gamma_0 < \gamma_B$, the time evolution of the electron distribution function is solely determined by the linear synchrotron losses, whereas for large injection parameters $\alpha > 1$, corresponding to $\gamma_0 > \gamma_B$, nonlinear SST losses determine the electron distribution function at early times.

2.2.2. Small injection energy $\gamma_0 < \gamma_B$

In the case of small injection energies $\gamma_0 < \gamma_B$ the injection parameter $\alpha < 1$ is smaller than unity, so that the arguments of the arctan-functions in Eq. (12) are always larger than unity. For all values of T and y Eq. (12) then simplifies to

$$T(y) \simeq K_0 y \quad (13)$$

In terms of y the solution (10) then reads $S(x, x_0, y) = q_0 H[x - x_0] \delta(x - x_0 - K_0 y)$, yielding

$$\begin{aligned} n(\gamma, \gamma_0, t) &= \frac{q_0}{\gamma^2} H[\gamma_0 - \gamma] \delta(\gamma^{-1} - \gamma_0^{-1} - D_0 t) \\ &= q_0 H[\gamma_0 - \gamma] \delta\left(\gamma - \frac{\gamma_0}{1 + D_0 \gamma_0 t}\right), \end{aligned} \quad (14)$$

which agrees with the standard linear synchrotron cooling solution (4).



Introduction

Linear synchrotron ...

Intrinsic optically ...

Synchrotron and ...

Comparison with ...

Summary and ...

2.2.3. High injection energy $\gamma_0 > \gamma_B$

In the case of high injection energies $\gamma_0 > \gamma_B$ the injection parameter $\alpha > 1$ is larger than unity. We rewrite Eq. (12) as

$$K_0 y + C_1 = \alpha x_0 \left[\frac{1 + \frac{T}{x_0}}{\alpha} - \arctan \left(\frac{1 + \frac{T}{x_0}}{\alpha} \right) \right] \quad (15)$$

For small times $0 \leq T \leq T_c$, where $T_c = (\alpha - 1)x_0$, we use $\arctan(x) \simeq x - (x^3/3)$ to obtain

$$K_0 y_1 + C_1 \simeq \frac{x_0}{3\alpha^2} \left(1 + \frac{T}{x_0} \right)^3, \quad (16)$$

and with $T(y_1 = 0) = 0$

$$y_1 = \frac{(x_0 + T)^3}{3q_0} - \frac{x_0^3}{3q_0} \quad (17)$$

This solution is valid for $T \leq T_c$, corresponding to

$$0 \leq y \leq y_c = \frac{x_0^3}{3q_0} (\alpha^3 - 1) = \frac{x_0}{3\alpha^2 K_0} (\alpha^3 - 1) \quad (18)$$



Introduction

Linear synchrotron . . .

Intrinsic optically . . .

Synchrotron and . . .

Comparison with . . .

Summary and . . .

For times $T \geq T_c$ or $y \geq y_c$ the argument of the arctan-function in Eq. (15) is large compared to unity, yielding the linear relation

$$y_2 = \frac{x_0 + T}{K_0} - C_4 \quad (19)$$

The constant C_4 is determined by the equality of the two solutions $y_1(T_c) = y_2(T_c) = y_c$ at T_c providing

$$y_2 = \frac{x_0 + T}{K_0} - \frac{2q_0^{1/2}}{3K_0^{-3/2}} - \frac{x_0^3}{3q_0} \quad (20)$$

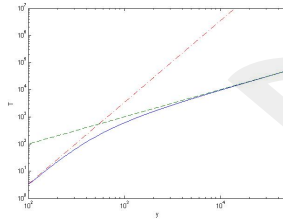


Figure 1: Comparison of exact solution $y(T)$ (full curve) with asymptotic solution $y_1(T)$ at small times (dashed curve) and asymptotic solution $y_2(T)$ at late times (dotted curve).



Introduction

Linear synchrotron . . .

Intrinsic optically . . .

Synchrotron and . . .

Comparison with . . .

Summary and . . .

Both approximate solutions (17) and (20) can be inverted to yield

$$T_1(y < y_c) = [3q_0y + x_0^3]^{1/3} - x_0 = x_0 \left[\left(1 + \frac{3\alpha^2 K_0 y}{x_0} \right)^{1/3} - 1 \right] \quad (21)$$

and

$$T_2(y \geq y_c) = x_0 \left[\frac{1}{3\alpha^2} \left(\frac{3\alpha^2 K_0 y}{x_0} + 1 + 2\alpha^3 \right) - 1 \right] \quad (22)$$

We then find for small times

$$n_1(\gamma, \gamma_0, t < t_c) = q_0 H[\gamma_0 - \gamma] H[t_c - t] \delta \left(\gamma - \frac{\gamma_0}{(1 + 3q_0 \gamma_0^3 A_0 t)^{1/3}} \right), \quad (23)$$

which agrees with the nonlinear SST solution of Schlickeiser (2009). At late times

$$n_2(\gamma, \gamma_0, t \geq t_c) = q_0 H[\gamma_B - \gamma] H[t - t_c] \delta \left(\gamma - \frac{\gamma_B}{\frac{1+2\alpha^3}{3\alpha^3} + \gamma_B K_0 A_0 t} \right), \quad (24)$$

which is a modified linear cooling solution. Note that both solution show that at time



Introduction

Linear synchrotron ...

Intrinsic optically ...

Synchrotron and ...

Comparison with ...

Summary and ...

$$\begin{aligned}
 t_c &= \frac{y_c}{A_0} = \frac{\alpha^3 - 1}{3\alpha^3 \gamma_B D_0} \simeq \frac{1}{3\gamma_B D_0} \\
 &= \frac{2.6 \cdot 10^8}{\gamma_B b^2} \text{ s} = \frac{1.2 \cdot 10^6 N_{50}^{1/2}}{R_{15} b^2} \text{ s}
 \end{aligned} \tag{25}$$

the electrons have cooled to the characteristic Lorentz factor γ_B .

2.2.4. Interlude

Summarizing this section: provided electrons are injected with Lorentz factors higher than γ_B , they initially cool down to the characteristic Lorentz factor γ_B by nonlinear SST-cooling until time t_c . At later times they further cool to lower energies according to the modified cooling solution (24). If the electrons are injected with Lorentz factors smaller than γ_B they undergo only linear synchrotron cooling at all energies with no influence of the SST cooling. The characteristic Lorentz factor γ_B is only determined by the injection conditions, whereas the time scale t_c also depends on the magnetic field strength.

This different cooling behaviour for large and small injection energies affects the synchrotron and SSC intensities and fluences which we investigate in the next sections.



Introduction

Linear synchrotron . . .

Intrinsic optically . . .

Synchrotron and . . .

Comparison with . . .

Summary and . . .

3. Intrinsic optically thin synchrotron radiation intensities and fluences

The optically thin synchrotron intensity $n(\gamma, t)$ is given by

$$I(\epsilon, t) = Rj_S(\epsilon, t) = \frac{R}{4\pi} \int_0^\infty d\gamma n(\gamma, t) p_S(\epsilon, \gamma), \quad (26)$$

In order to collect enough photons, intensities are often averaged or integrated over long enough time intervals. For rapidly varying photon intensities this corresponds to fractional fluences which are given by the time-integrated intensities $F_f(\epsilon, t_f) = \int_0^{t_f} dt I(\epsilon, t)$. The total fluence spectra result in the limit $t_f \rightarrow \infty$

$$F(\epsilon) = F_f(\epsilon, t_f = \infty) = \int_0^\infty dt I(\epsilon, t) = \frac{1}{3A_0 q_0 \gamma_0^3} \int_0^\infty d\tau I(\epsilon, \tau) \quad (27)$$

For small injection energy ($\alpha \ll 1$) we obtain

$$F_s(\epsilon) \simeq F_{0S} \begin{cases} c_0 \left(\frac{E_0}{\epsilon}\right)^{1/2} & \text{for } \epsilon \ll E_0, \\ \left(\frac{E_0}{\epsilon}\right) \exp(-\epsilon/E_0) & \text{for } \epsilon \gg E_0. \end{cases} \quad (28)$$

whereas for large ($\alpha \gg 1$) we find



Introduction

Linear synchrotron ...

Intrinsic optically ...

Synchrotron and ...

Comparison with ...

Summary and ...

$$F_h(\epsilon) \simeq F_{0h} \begin{cases} c_0 \alpha^2 \left(\frac{E_0}{\epsilon}\right)^{1/2} & \text{for } \epsilon \ll E_0/\alpha^2, \\ c_2 \left(\frac{E_0}{\epsilon}\right)^{3/2} & \text{for } E_0/\alpha^2 \ll \epsilon \ll E_0, \\ \left(\frac{E_0}{\epsilon}\right) \exp(-\epsilon/E_0) & \text{for } \epsilon \gg E_0. \end{cases} \quad (29)$$

For the total fluence SED $S(\epsilon) = \epsilon F(\epsilon)$ we then find in the two cases of small (s) and high (h) injection energies

$$S_s(\epsilon) = S_0 \frac{\alpha^2}{\gamma_0} \left(\frac{\epsilon}{E_0}\right)^{1/2} \exp(-\epsilon/E_0) \quad (30)$$

and

$$S_h(\epsilon) = S_0 \frac{\alpha^2}{\gamma_0} \left(\frac{\epsilon}{E_0}\right)^{1/2} \frac{\epsilon_B}{\epsilon + \epsilon_B} \exp(-\epsilon/E_0), \quad (31)$$

with the constant $S_0 = 3c_0 mc^2 / 32c_1 \sigma_T$ and the characteristic break energy

$$\epsilon_B = \frac{c_2 E_0}{c_0 \alpha^2} = 0.703 \frac{E_0}{\alpha^2} \quad (32)$$

The ratio of peak values is given by

$$\mathcal{R} = \frac{N_{h,peak}}{N_{s,peak}} \simeq 0.97 \frac{\alpha_h}{\alpha_s^2} \quad (33)$$



Introduction

Linear synchrotron ...

Intrinsic optically ...

Synchrotron and ...

Comparison with ...

Summary and ...

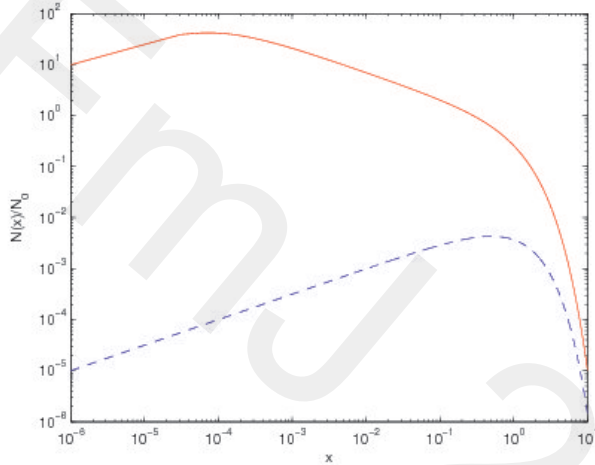


Figure 2: Total synchrotron fluence SED $N(x)$ as a function of $x = \epsilon/E_0$ for high ($\alpha_h = 100$, full curve) and small ($\alpha_s = 0.1$, dashed curve) injection conditions calculated for $\gamma_0 = 10^4$.



Introduction

Linear synchrotron ...

Intrinsic optically ...

Synchrotron and ...

Comparison with ...

Summary and ...

3.1. Summary of the differences

D1) In the high injection case the synchrotron SED peaks at a photon energy which is a factor $2x_B = 1.4\alpha_h^2 = 1.4 \cdot 10^{-4}$ smaller than the peak in the small injection case.

D2) The high injection energy peak value decreases at small times $t < \alpha t_s/3$ more rapidly than the small injection energy peak value.

D3) The high injection SED is a broken power law with spectral indices $+0.5$ below and -0.5 above the peak energy $x_B \ll 1$, respectively, and it cuts-off exponentially at photon energies $x > 1$. Below the peak energy x_B the time of maximum synchrotron intensity decreases as $t_{\max} \propto \epsilon^{-1/2}$, whereas above the peak energy x_B it decreases more rapidly as $t_{\max} \propto \epsilon^{-3/2}$ due to the severe additional SST losses.

D4) The small injection SED is a single power law with spectral indices $+0.5$ below the peak energy 0.5 , and it cuts-off exponentially at photon energies $x > 1$. Here the time of maximum synchrotron intensity decreases as $t_{\max} \propto \epsilon^{-1/2}$ at all energies $x < 1$ because in the small injection case the SST-losses do not contribute.

These predicted differences for the total synchrotron fluence SED and the synchrotron light curve behaviours provides a conclusive test for the presence of high or low injection energy conditions in blazars.



Introduction

Linear synchrotron ...

Intrinsic optically ...

Synchrotron and ...

Comparison with ...

Summary and ...

4. Synchrotron and SSC fluence SEDs from numerical radiation code

In Figs. 3 and 4 we show the synchrotron and SSC SEDs calculated with the numerical radiation code of Böttcher et al. (1997) using a magnetic field strength $b = 1$ and an injection Lorentz factor $\gamma_0 = 10^4$ for the high ($\alpha_h = 100$) and small ($\alpha_s = 0.1$) injection case.

Both synchrotron SEDs are in remarkable agreement with the analytical SEDs shown in Fig. 2. In particular, the numerical SEDs confirm all four predicted differences listed in the last section. For orientation, we have plotted in both figures the asymptotic analytical synchrotron spectra as dashed and dash-dotted lines.



Introduction

Linear synchrotron . . .

Intrinsic optically . . .

Synchrotron and . . .

Comparison with . . .

Summary and . . .

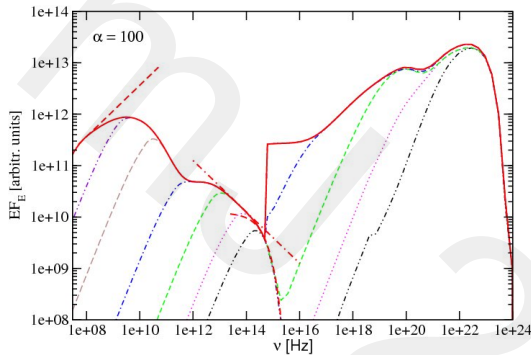


Figure 3: Numerically calculated fractional and total synchrotron and SSC fluence SEDs for high ($\alpha_h = 100$) injection conditions calculated for $\gamma_0 = 10^4$. Note that the SSC emission has been artificially cut off at low frequencies as it would otherwise overwhelm the high-energy end of the synchrotron emission.



Introduction

Linear synchrotron ...

Intrinsic optically ...

Synchrotron and ...

Comparison with ...

Summary and ...

The radiation code also yields the SSC fluence SEDs. We note from Figs. 3 and 4 that for the high injection case the SSC SED has a much higher amplitude than the synchrotron SED, whereas the opposite holds for the low injection case. Moreover, both SSC SEDs peak at the same photon energy, although the SSC peak value in the high injection case is a factor $2 \cdot 10^7$ larger than in the small injection case.

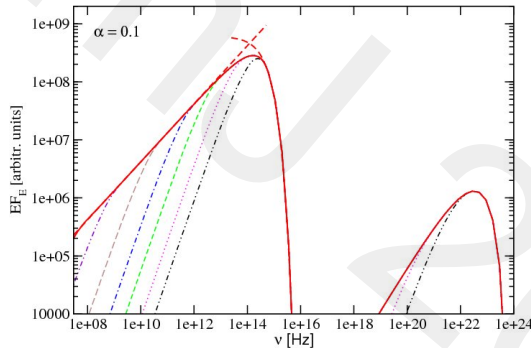


Figure 4: Numerically calculated fractional and total synchrotron and SSC fluence SEDs for small ($\alpha_s = 0.1$) injection conditions calculated for $\gamma_0 = 10^4$. The full curves show the total fluence SEDs. The dashed lines show the analytical asymptotes.



Introduction

Linear synchrotron ...

Intrinsic optically ...

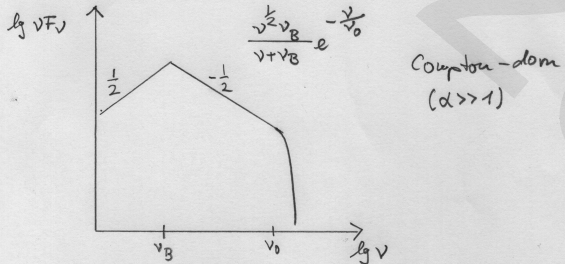
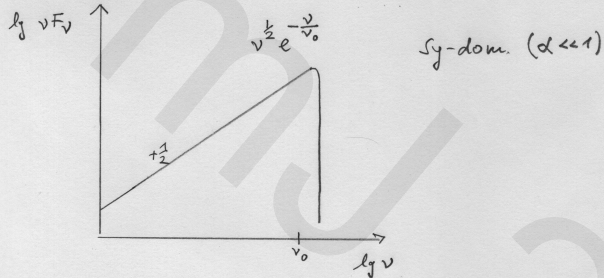
Synchrotron and ...

Comparison with ...

Summary and ...

Prediction for total synchrotron flux SED

for initial ($t=0$) injection of mono-energetic electrons $\gamma_0 = 10^4 \gamma_4$:



$$\nu_0 = 2.4 \cdot 10^{14} \gamma_4^2 \text{ Hz}, \quad \nu_B = \frac{\nu_0}{\alpha^2}$$

$$\text{Injection parameter: } \alpha = \frac{\gamma_0}{\gamma_B} = \frac{46 \gamma_4 N_{50}^{\frac{1}{2}}}{R_{15}}$$

$$\gamma_B = \frac{217 R_{15}}{\nu}$$



Introduction

Linear synchrotron ...

Intrinsic optically ...

Synchrotron and ...

Comparison with ...

Summary and ...

5. Comparison with observations and future work

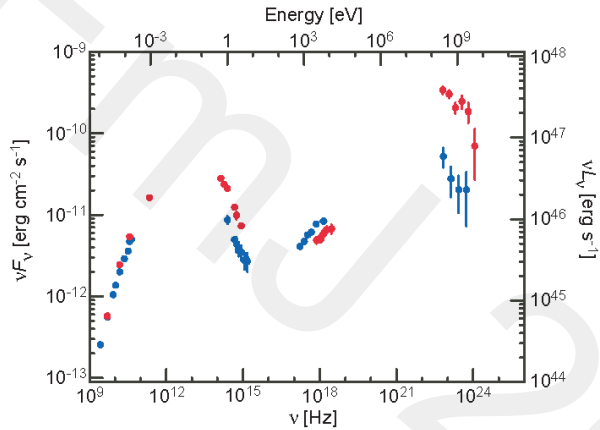


Figure 5: Compton-dominated source 3C 279



Introduction

Linear synchrotron ...

Intrinsic optically ...

Synchrotron and ...

Comparison with ...

Summary and ...

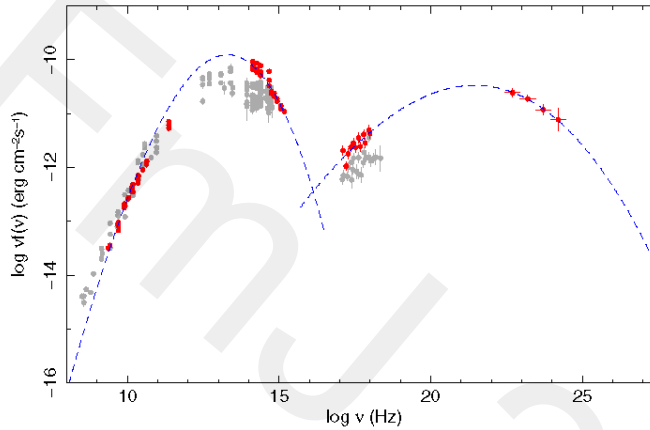


Figure 6: Synchrotron-dominated source PKS0851+202 from Fermi survey

Differences in the synchrotron fluence SEDs in agreement with predictions!



Introduction

Linear synchrotron ...

Intrinsic optically ...

Synchrotron and ...

Comparison with ...

Summary and ...

5.1. Future work

- Analytical behavior of SSC fluence SEDs for small and large injection parameter α (BSc thesis M. Mandelartz)
- Corresponding analysis for power law injection $q \propto \gamma^{-s}, \gamma_1 \leq \gamma \leq \gamma_2$ (PhD thesis M. Zacharias): no significant differences as compared to monoenergetic injection because of rapid quenching of power-law.
- Meeting Jansky: influence of optically thickness on low-frequency synchrotron intensity and fluence SEDs (BSc thesis V. Friedhoff)



Introduction

Linear synchrotron . . .

Intrinsic optically . . .

Synchrotron and . . .

Comparison with . . .

Summary and . . .

6. Summary and conclusions

- The broadband SEDs of blazars exhibit two broad spectral components which in leptonic emission models are attributed to synchrotron radiation and SSC radiation of relativistic electrons. If the high-frequency SSC component dominates over the low-frequency synchrotron component, the inverse Compton SSC losses of electrons are at least equal or greater than the synchrotron losses of electrons. The linear synchrotron cooling, included standardly in radiation models of blazars, then has to be supplemented by the SSC cooling.
- The SSC energy loss rate of electrons calculated in the Thomson limit (SST cooling) exhibits nonlinear behaviour because it depends on an energy integral of the actual electron spectrum, reflecting the dependence of the energy density of the target synchrotron photons on the differential electron energy spectrum. The dependence on the initial kinetic energy of injected electrons is a collective effect completely different from the linear synchrotron case.
- For the illustrative case of instantaneous injection of monoenergetic particles we solve the nonlinear kinetic equation for the intrinsic temporal evolution of the relativistic particles under combined linear synchrotron and nonlinear SST-cooling.



Introduction

Linear synchrotron . . .

Intrinsic optically . . .

Synchrotron and . . .

Comparison with . . .

Summary and . . .



- Qualitatively differences for the light curves and SEDs resulting depending on whether electron cooling is initially Compton dominated (high injection energy parameter α) or it is always synchrotron dominated (low α). The injection parameter parameter $\alpha = \gamma_0/\gamma_B$ depends on the Lorentz factor γ_0 of injected electrons energy density of the initially injected relativistic electrons and can be written as and the characteristic Lorentz factor $\gamma_B = 217R_{15}N_{50}^{-1/2}$, fixed by the source radius $R = 10^{15}R_{15}$ cm and the total number of instantaneously injected electrons $N = 10^{50}N_{50}$.
- In the low- α case, the resulting fluence spectrum exhibits a simple exponentially cut-off power-law behaviour, $S_\nu \propto \nu^{1/2}e^{-\nu/\nu_0}$. In contrast, in the high- α case, we find a broken power-law with exponential cutoff, parametrized in the form $S_\nu \propto \nu^{1/2} \frac{\nu_B}{\nu + \nu_B} e^{-\nu/\nu_0}$. Based on our analysis we propose the following interpretation of multiwavelength blazar SEDs:
- Blazars, where the γ -ray fluence is much larger than the synchrotron fluence, are regarded as high injection energy sources. Here, the synchrotron fluence should exhibit the symmetric broken power law behaviour around the synchrotron peak energy that is a factor $(\alpha_h \gamma_0)^2$ smaller than the SSC peak energy. Below and above ν_B the synchrotron light curve peak times exhibit different frequency dependences $t_{\max}(\nu < \nu_B) \propto \nu^{-1/2}$ and $t_{\max}(\nu > \nu_b) \propto \nu^{-3/2}$, respectively, resulting from the additional severe SST-losses at $\nu > \nu_B$.

Introduction

Linear synchrotron ...

Intrinsic optically ...

Synchrotron and ...

Comparison with ...

Summary and ...

- Blazars, where the γ -ray fluence is much smaller than the synchrotron fluence, are regarded as small injection energy sources. Here, the synchrotron fluence exhibits the single power law behaviour (D4) up to a higher synchrotron peak energy that is a factor γ_0^2 smaller than the SSC peak energy. In this case the synchrotron light curve peak time exhibits the standard linear synchrotron cooling decrease $t_{\max}(\nu) \propto \nu^{-1/2}$ at all frequencies.
- If the injection Lorentz factor γ_0 and the size of the source are the same, different values of the injection parameter α result from different total numbers of instantaneously injected electrons. E.g., the high injection case $\alpha_h = 100$ results for $N_{50} = 4.7$, whereas the low injection case $\alpha_s = 0.1$ needs $N_{50} = 4.7 \cdot 10^{-6}$.
- These predictions of spectral behaviour with time and frequency provide conclusive tests for the presence or absence of linear synchrotron cooling or nonlinear SST cooling in flaring nonthermal sources.



Introduction

Linear synchrotron . . .

Intrinsic optically . . .

Synchrotron and . . .

Comparison with . . .

Summary and . . .

Thanks to

- Ulf Menzler, Michael Zacharias (Ruhr-Universität Bochum)
- Markus Böttcher (Ohio University)
- The HESS-Team
- Deutsche Forschungsgemeinschaft (Schl 201/23-1, Schl 201/20-1)



bmb+f - Förderschwerpunkt

Astroteilchenphysik

Großgeräte der physikalischen
Grundlagenforschung



Introduction

Linear synchrotron . . .

Intrinsic optically . . .

Synchrotron and . . .

Comparison with . . .

Summary and . . .